Journal of Geophysical Research: Space Physics

RESEARCH ARTICLE
10.1029/2018JA025797

The Acceleration of Electrons to High Energies Over the Jovian Polar Cap via Whistler Mode Wave-Particle Interactions

S. S. Elliott[1], D. A. Gurnett[1], W. S. Kurth[1], B. H. Mauk[2], R. W. Ebert[3], G. Clark[2], P. Valek[3], F. Allegrini[3,4], and S. J. Bolton[3]

[1]Department of Physics and Astronomy, University of Iowa, Iowa City, IA, USA, [2]The Johns Hopkins University Applied Physics Laboratory, Laurel, MD, USA, [3]Southwest Research Institute, San Antonio, TX, USA, [4]Department of Physics and Astronomy, University of Texas at San Antonio, San Antonio, TX, USA

Key Points:
- Upgoing energetic electrons with power law-like spectrums and strong upgoing whistler mode waves are observed over the Jovian polar cap
- The upgoing broadband whistler mode waves are generated by an electron beam instability at low altitudes in the upper ionosphere
- The upgoing electrons are stochastically accelerated by the broadband whistler mode waves via the development of Hamiltonian chaos

Correspondence to:
S. S. Elliott,
sadie-tetrick@uiowa.edu

Citation:
Elliott, S. S., Gurnett, D. A., Kurth, W. S., Mauk, B. H., Ebert, R. W., Clark, G., et al. (2018). The acceleration of electrons to high energies over the Jovian polar cap via whistler mode wave-particle interactions. *Journal of Geophysical Research: Space Physics*, *123*, 7523–7533. https://doi.org/10.1029/2018JA025797

Received 18 JUN 2018
Accepted 23 AUG 2018
Accepted article online 30 AUG 2018
Published online 22 SEP 2018

Abstract Upward traveling electrons with energies from tens of kiloelectron volts to several megaelectron volts have been observed over the Jovian polar regions in association with intense upward propagating whistler mode waves. The electrons have a power law-like energy distribution, indicative of a stochastic acceleration process. The energy flux of the upward propagating whistler mode waves is comparable to and strongly correlated with the energy flux of the upward traveling energetic electrons, suggesting that the whistler mode waves may be accelerating the electrons. We propose that a downward field-aligned current over the polar cap generates strong downward parallel electric fields and associated upward electron beams in the low-density regions of Jupiter's upper ionosphere, a mechanism similar to the formation of inverted-Vs in Earth's auroral regions. At Jupiter, the upward-traveling electron beams produce intense upward propagating whistler mode emissions over a broad frequency range, similar to upward propagating auroral hiss at Earth. As the whistler mode waves propagate upward out of the inverted-V source region, the waves are absorbed by the plasma, thereby accelerating the electrons. We attribute the stochastic power law-like energy spectrum of the accelerated electrons to the development of Hamiltonian chaos (velocity space diffusion), the signature of which is indicated by the occurrence of spiky soliton-like variations in the whistler mode electric fields. Acceleration to high energies may be facilitated by the rapid increase in the phase velocity of the whistler mode waves with increasing altitude, which could accelerate some of the electrons trapped in the wavefield to very high relativistic energies.

1. Introduction

One of the most exciting discoveries recently made by the Juno spacecraft is the observation of upward traveling energetic electrons (from tens of kiloelectron volts to above 1 MeV), presumably on open field lines, over the Jovian polar cap (Allegrini et al., 2017; Connerney et al., 2017; Mauk, Haggerty, Paranicas, et al., 2017; Paranicas et al., 2018). The observation was made by the Jupiter Energetic-particle Detector Instrument (JEDI; Mauk, Haggerty, Jaskulek, et al., 2017) and the Jovian Auroral Distributions Experiment (JADE; McComas et al., 2017). The energy spectra of the electrons have nearly power law distributions (Figure 1), suggesting a stochastic acceleration process (Ma & Summers, 1998). The Juno Waves instrument (Kurth et al., 2017) also detected intense upward propagating broadband whistler mode waves over the entire Jovian polar cap region (Tetrick et al., 2017). These whistler mode waves are analogous to auroral hiss at Earth, which is known to be generated by beams of electrons called inverted-Vs (Frank & Ackerson, 1971; Gurnett, 1972; Gurnett & Frank, 1972; Gurnett et al., 1983). The upward propagating whistler mode waves and the upward traveling electrons at Jupiter are positively correlated, and the electrons show evidence of substantial pitch angle scattering via wave-particle interactions (Elliott et al., 2018). Also, the energy flux of the electrons and waves is roughly comparable over the polar cap (within a factor of 10), suggesting that the waves may play an important role in the electron acceleration. Here we provide the first detailed theoretical and quantitative analysis of this idea. We propose a unifying theory for the acceleration of upward traveling polar cap electrons that involves a mechanism similar to the wave-particle interactions that occur in a linear accelerator.

2. Wave Growth and Electron Acceleration

There are two primary potential sources of energy that can drive planetary magnetospheric phenomena: interactions with the solar wind and interactions with the rotation of the planet. Jupiter's primary energy

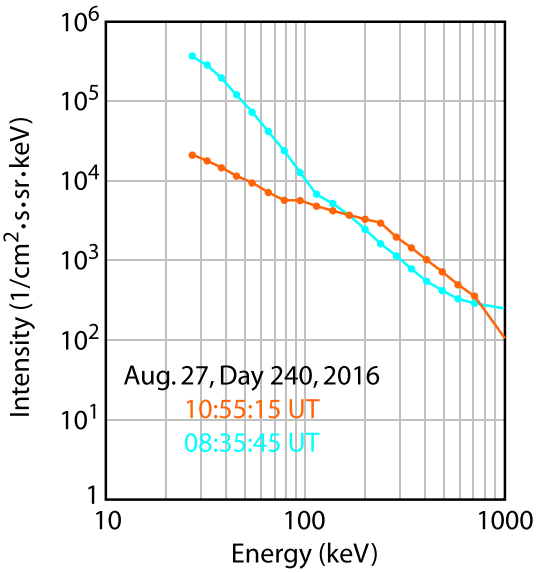

Figure 1. Example energy spectra for upward traveling electrons over the polar cap during perijove 1, demonstrating power law-like distributions (adapted from Mauk, Haggerty, Paranicas, et al., 2017).

source is widely thought to be dominated by the rapid rotation of the planet, and we adopt this point of view. In Figure 2 we show a simplified Homopolar generator (Pugh & Pugh, 1965) model that can be used to understand the *big picture* of the Jovian current system and how it drives upward traveling electrons in the polar cap. As the conducting disk rotates, an electromotive force is induced, producing a current that is directed outward at the equator. This current must then close along the polar cap field lines, resulting in a downward current over the polar cap. Magnetic field measurements show that a current of approximately 7×10^7 A enters each of Jupiter's polar caps (Connerney, 1981). This current is ultimately driven by the transfer of angular momentum to outflowing mass in the equatorial plane (Hill, 1979). The black box in Figure 2 represents the polar observations made by Juno, including the upward traveling energetic electrons and the upward propagating whistler mode waves. Specifically, it symbolizes the important open question regarding whether whistler mode waves, driven by the field-aligned current, can accelerate the electrons to megaelectron volt energies. Answering this question is the focus of this paper.

Inside the sketched black box in Figure 2 is the letter *E*, referring to a parallel electric field, which can drive a beam-plasma instability. Where this electric field and the associated beam-plasma instability occurs is determined by the following considerations. The electron density in the region above the ionosphere often drops to very low levels, sometimes providing too few electrons to carry the downward plasma current. This effect is further reinforced by the convergence of the magnetic field lines near the planet, which increases the local current density, making it even more difficult for the plasma to carry the required current (Mozer & Hull, 2001). Because the current is carried primarily by the electrons, the electron drift velocity relative to ion velocity, $|V_e - V_i|$, is the crucial parameter that determines the current density. Figure 3 shows that this drift velocity increases, reaches a peak, and then decreases as a function of altitude. In the region near the peak, the drift velocity may reach a threshold, above which there are not enough electrons to carry the required current density. This threshold is at or near the electron thermal velocity, $|V_e - V_i| > V_{\text{th}}$. If the threshold is exceeded, which is often believed to be the case, then a parallel electric field develops that creates a beam of electrons that maintains the current system driven by the Homopolar generator (which acts as a constant current source). It is this beam of electrons that is the source of the upward propagating whistler mode auroral hiss.

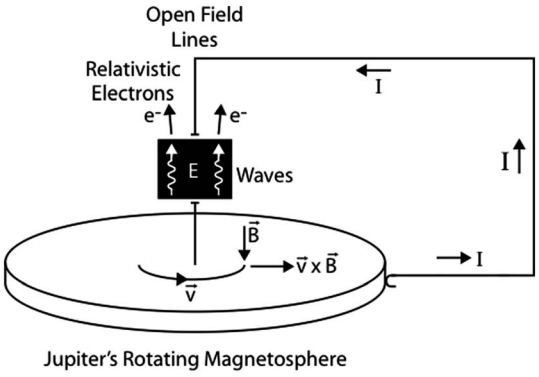

Figure 2. The Homopolar generator model applied to the Jovian current system. A $-\vec{v}\times\vec{B}$ force induces an electromotive force, producing an outward radial current that must close as a downward current over the polar cap. Because we believe these are open field lines, the current closes through the solar wind.

To analyze the growth rate, γ, of waves generated by the beam, we use equation 10.3.39 from Gurnett and Bhattacharjee (2017), which is for wave propagation parallel to the magnetic field,

$$\gamma = \pi \frac{1}{\partial D_r/\partial\omega}\left[\frac{\omega_p^2}{\omega^2}\left[-\frac{\omega}{|k_\parallel|}\int_0^\infty F_0 2\pi v_\perp dv_\perp - \frac{k_\parallel}{|k_\parallel|}\int_0^\infty\left(v_\parallel\frac{\partial F_0}{\partial v_\perp} - v_\perp\frac{\partial F_0}{\partial v_\parallel}\right)\pi v_\perp^2 dv_\perp\right]\right]\Bigg|_{v_\parallel = v_{\parallel\text{res}} = \frac{\omega - n\omega_c}{k_\parallel}} \quad (1)$$

where D_r is the real part of the dispersion relation, F_0 is the normalized electron velocity distribution function, ω_p is the plasma frequency, ω_c is the cyclotron frequency, and $v_\perp$ and $v_\parallel$ represent perpendicular and parallel electron velocities, respectively. Although strictly valid only for waves propagating exactly along the magnetic field, since most of the whistler mode waves detected by Juno are propagating at relatively small angles to the magnetic field, we believe that this growth rate equation gives a reasonable first-order approximation. The growth rate,

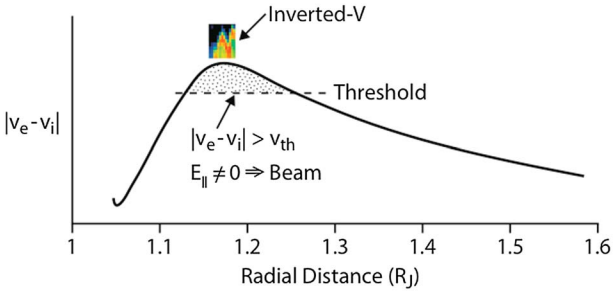

Figure 3. Plot of the electron velocity relative to the ion velocity as a function of radial distance, showing a region where this velocity shift is high enough to develop a parallel electric field (i.e., an electron beam or inverted-V). A combination of both the density not being high enough to carry the necessary downward current and the convergence of the magnetic field lines causes a parallel electric field to develop.

γ, in equation (1) can be positive or negative, representing wave growth or wave damping, respectively. Examination of the equation shows that it contains the following three important terms:

(1) $-\frac{\omega}{|k_{\parallel}|}\int_0^{\infty} F_0 2\pi v_{\perp} dv_{\perp}$

(2) $-\int_0^{\infty}\left(v_{\parallel}\frac{\partial F_0}{\partial v_{\perp}}\right)\pi v_{\perp}^2 dv_{\perp}$

(3) $+\int_0^{\infty}\left(v_{\perp}\frac{\partial F_0}{\partial v_{\parallel}}\right)\pi v_{\perp}^2 dv_{\perp}$

The first term is proportional to the number of resonant electrons and always contributes to damping. The second term depends on the derivative of the electron velocity distribution function in the perpendicular direction, and the third term depends on the derivative of the electron velocity distribution function in the parallel direction. To model the electron beam, we used a simple Maxwellian distribution function (Figure 4). There are three possible categories of values for the integer n in the resonance condition for equation (1): positive, zero, and negative. Each value for n reflects a different combination of polarization and direction of propagation for the waves and resonant particles (Kennel & Wong, 1967). In radiation belt physics, the $n = +1$, or the cyclotron resonance condition, is commonly used because the waves and the resonant electrons in radiation belt physics are always moving in opposite directions. However, the Juno observations over the polar cap region show that the electrons and waves are moving in the same direction (upward), so the interaction must involve either zero or negative values of n. Negative n cases deal with ion resonances, which we believe to be of negligible importance in this study. Therefore, we limit our analysis to the $n = 0$ case, often called the Landau resonance.

When we incorporate the $n = 0$ Landau resonance condition into equation (1) and carry out the integration in the second term, we discover that the second term cancels the first term (see the appendix for a full derivation). This result leaves us with the third term as the only important term in the summation:

$$+\int_0^{\infty}\left(v_{\perp}\frac{\partial F_0}{\partial v_{\parallel}}\right)\pi v_{\perp}^2 dv_{\perp}$$

This term can either be positive or negative, depending on the sign of $(\partial F_0/\partial v_{\parallel})$. Inspection of Figure 4 shows that for a Gaussian-like beam this partial derivative term is positive on the left-hand side of the distribution function (blue region), causing wave growth, and becomes negative on the right-hand side (pink region), resulting in wave damping. Note that damping means electron acceleration, the details of which are discussed later. The *tipping point* (from positive to negative γ) is determined by the wave phase velocity relative to the average electron beam velocity. As the phase velocity of the wave increases, it surpasses the average beam velocity. The distribution function then reaches a peak and starts decreasing, resulting in wave damping.

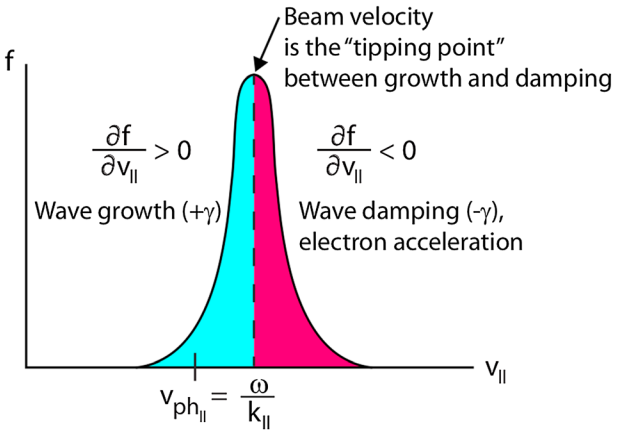

Figure 4. Maxwellian distribution function for an electron beam in the parallel direction. The blue region indicates wave growth, and pink indicates wave damping and electron acceleration. The average electron beam velocity relative to the wave phase velocity determines the *tipping point*.

Because the wave phase velocity (V_{ph}) is proportional to the inverse of the index of refraction, one can examine the conditions placed on the parallel electron beam velocity ($V_{\parallel Beam}$) to create an instability. Figure 5 shows a representative index of refraction plot for the whistler mode (panel a) and the associated V_{ph} plot (panel b). In Figure 5b, the horizontal dashed line, labeled $V_{\parallel Beam}$, represents a possible beam velocity. This illustration demonstrates that an upper limit exists for the beam velocities that can generate whistler mode waves, which is a standard principle of Landau acceleration and damping. If the beam velocity is too high, no intersection point (resonance) occurs and whistler mode waves cannot be generated. We estimated this upper cutoff to be ~300 keV by using the index of refraction for the whistler mode waves. Figure 5b also shows that $V_{\parallel Beam}$

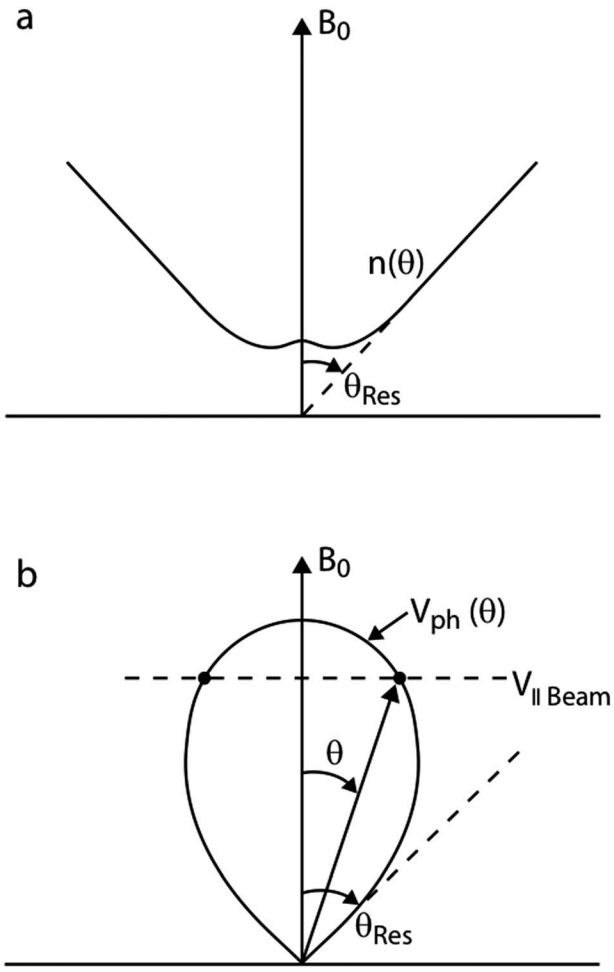

Figure 5. (a) The index of refraction for the whistler mode in low density regime ($f_{pe} \ll f_{ce}$). (b) Associated wave phase velocity (V_{ph}) for the whistler mode. The horizontal dashed line indicates a possible beam velocity ($V_{\|\,Beam}$), showing two intersection points (resonances). The resonance cone (θ_{res}) shows a region where the waves become quasi-electrostatic. Our whistler mode waves are not propagating along the resonance cone and are therefore electromagnetic.

intersections are relatively close to the magnetic field. The resonance cone (θ_{res}) represents the limiting angle at which the whistler mode can propagate. Along this angle, the index of refraction goes to infinity and the whistler mode waves become quasi-electrostatic. At Earth, whistler mode auroral hiss is known to propagate nearly along the resonance cone and is quasi-electrostatic, with little or no magnetic wavefield. However, the Jovian polar cap whistler mode emissions are propagating more nearly along the magnetic field and usually not near the resonance cone (Tetrick et al., 2017). This is a consequence of the very strong planetary magnetic field at Jupiter ($\omega_c \gg \omega_p$), which makes the whistler mode index of refraction much smaller than at Earth (near one and more electromagnetic, less electrostatic).

As was stated earlier, the tipping point in the electron beam distribution function is determined by the phase velocity. In order to model the wave phase velocity, we need both an ionospheric density model and a magnetospheric density model (Figure 6a). For the ionosphere, we used a simple Chapman model (Chapman, 1931) and for the magnetosphere we used a constant magnetospheric density ($n_e \approx 20$ cm^{-3}), which is consistent with the electron plasma frequency (~40 kHz) determined by Tetrick et al. (2017). We justify the use of a simple Chapman ionospheric density model by the fact that the overall resulting behavior of the wave phase velocity to increase would not be affected by more complicated electron density profiles. A simple dipole magnetic field model was also used to calculate the index of refraction as a function of radial distance (R_J). We then converted the index of refraction to phase velocity using the following equation:

$$v_{ph\|} = \frac{c}{n}\cos\,\theta \tag{2}$$

where $v_{ph\|}$ is the parallel phase velocity, c is the speed of light, n is the index of refraction, and θ is the angle relative to the magnetic field; for the latter calculation, we used the approximation that the waves are nearly field aligned.

Figure 6b shows the resulting phase velocity as a function of radial distance. The dashed line in the plot shows a 30-keV electron beam velocity, which is typical for an inverted-V at Jupiter. When the wave phase velocity is below this beam velocity, a beam-plasma instability can occur and cause whistler mode waves to grow. Because the phase velocity increases as altitude (or radial distance) increases, the wave phase velocity exceeds the electron beam velocity and reaches a tipping point where the waves are subsequently absorbed, causing electrons to be accelerated. The blue and pink colors in Figure 6b have the same representation as in Figure 4. A cartoon representation of this mechanism is shown in Figure 7, along with expected observations of both an inverted-V and upward propagating whistler mode waves.

3. Juno Wave and Particle Observations

Our proposed electron acceleration mechanism predicts that inverted-Vs should be detected at low altitudes, in the regions where the whistler mode waves are produced. As the altitude of the spacecraft increases, we expect a transition from a region of wave production ($\gamma > 0$) to a region of wave absorption and electron acceleration ($\gamma < 0$). Figure 8 shows Juno observations of the southern polar regions on 11 December 2016 (panels a, b, and d) and 27 March 2017 (panels c and e). Figures 8a and 8b show 0.1- to 100-keV electron observations from perijove 3 (Ebert et al., 2017), taken by the Jovian Auroral Distributions Experiment-Electron instrument (McComas et al., 2017). Characteristic arc-like energy time structures are observed,

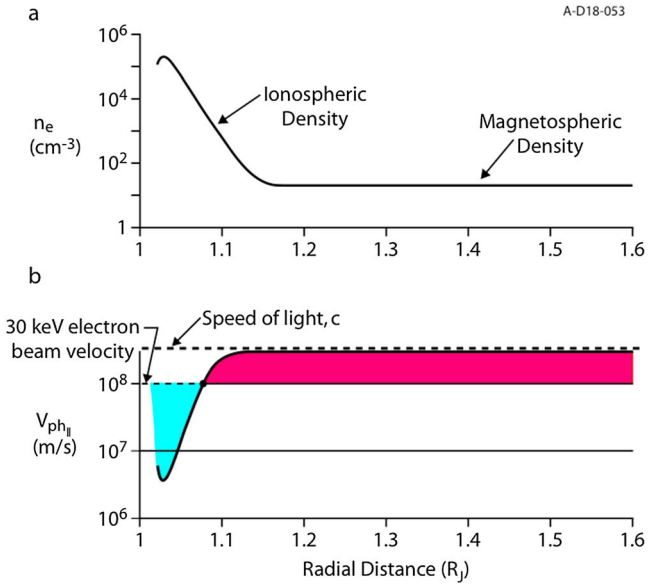

Figure 6. (a) Ionospheric density model (Chapman model with added magnetospheric constant density of $n_e \approx 20$ cm^{-3}). (b) Phase velocity as a function of radial distance. A beam velocity for a 30-keV electron beam and the speed of light are represented by dashed lines. Blue and pink colors indicate wave growth and wave damping, respectively (as in Figure 4).

with energy peaks ranging from 20 to >100 keV. These structures are interpreted as inverted-Vs, which are signatures of electron beam acceleration by parallel electric fields (Frank & Ackerson, 1971). Similarly, Figure 8c shows inverted-V electrons observed during perijove 5. These observations can be compared to upward propagating whistler mode wave observations taken by the Juno Waves instrument (Figures 8d and 8e). The Waves data can be interpreted as a radial/altitude profile, demonstrating that the inverted-V electrons are observed at low altitudes (Figure 8f). As the spacecraft moves to higher altitudes, the whistler mode waves are then absorbed and the wave energy is transferred into accelerating the electrons to high energies. Therefore, we believe that the upward propagating whistler mode waves observed over the polar cap (Figures 8d and 8e) are the remnant of waves that are responsible for the nearly relativistic upward traveling electrons.

Consistent with our prediction of wave production at low altitudes, Ebert et al. (2017) found an estimated range that the inverted-Vs were observed by the Jovian Auroral Distributions Experiment-Electron instrument instrument to be ~1.4 to 2.9 R_J. These radial distances are relatively small and support our theory that the wave generation is occurring at lower altitudes. It should also be noted that JEDI observed a higher energy inverted-V in the southern polar region during perijove 3 (peaking from ~30 up to ~300 keV; Clark et al., 2017). The inverted-V seen on JEDI also occurred at lower altitudes (roughly at 2.77 R_J), which is consistent with our proposed theory.

4. Stochastic Electron Acceleration

Our model must be able to explain how a broad range of electron energies can be produced (i.e., power law-like distributions, Figure 1). A viable mechanism for stochastic acceleration of electrons is chaotic motion of electrons driven by the broadband whistler mode waves. It is well known that Hamiltonian systems have the capability to exhibit chaotic behavior. Because the equation of motion for the electrons can be written as a Hamiltonian, it is expected that, for sufficiently intense waves, the system will transition into Hamiltonian chaos. The details and requirements for Hamiltonian chaos can be found in section 11.1.3 of Gurnett and Bhattacharjee (2017), but the main point is that an intense, broadband wave spectrum can lead to chaotic particle motions and strong velocity space diffusion. Because Juno observed a broad spectrum of intense whistler mode waves over the polar cap regions, chaotic motion of the electrons is likely, ultimately resulting in stochastic electron acceleration.

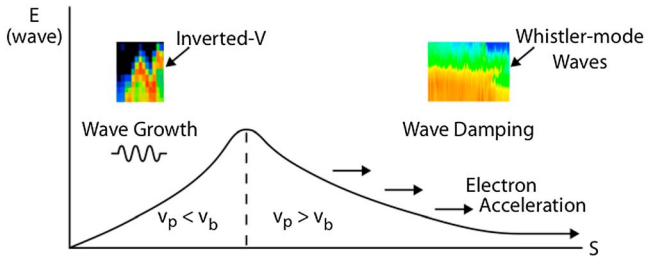

Figure 7. Cartoon representation of the wave electric field as the wave propagates along the field line (*S*). Initially, there is wave growth (when the phase velocity of the wave is less than the electron beam velocity) but when the tipping point is reached (when the phase velocity is larger than the beam velocity), the wave is damped and accelerates the electrons. Example Juno observations of an inverted-V (electron beam) and damped whistler mode waves are shown in their corresponding region along the magnetic field line.

One signature of chaotic motion, such as described above, is the presence of electrostatic solitary waves (ESWs), which are commonly observed in Earth's magnetosphere (e.g., Ergun et al., 1998; Mozer et al., 1997; Temerin et al., 1982). ESWs are the final state of the nonlinear evolution of an instability driven by an electron beam (Matsumoto et al., 1994). ESWs create large potential steps throughout the lifetime of an electron and can accelerate electrons to very high energies. Because ESWs are omnipresent in a variety of spacecraft observations, electrons moving along magnetic field lines can be accelerated by the sum of the individual potential drops, resulting in a broad range of electron energies (Mozer et al., 2014).

In Figure 9 we show the electric and magnetic waveforms for time periods corresponding to when Juno was over the polar cap. These waveforms demonstrate irregularities and structures similar to ESWs. However, the Jovian structures also contain a magnetic component, meaning that the waves are electromagnetic, similar to electromagnetic solitons (Biswas

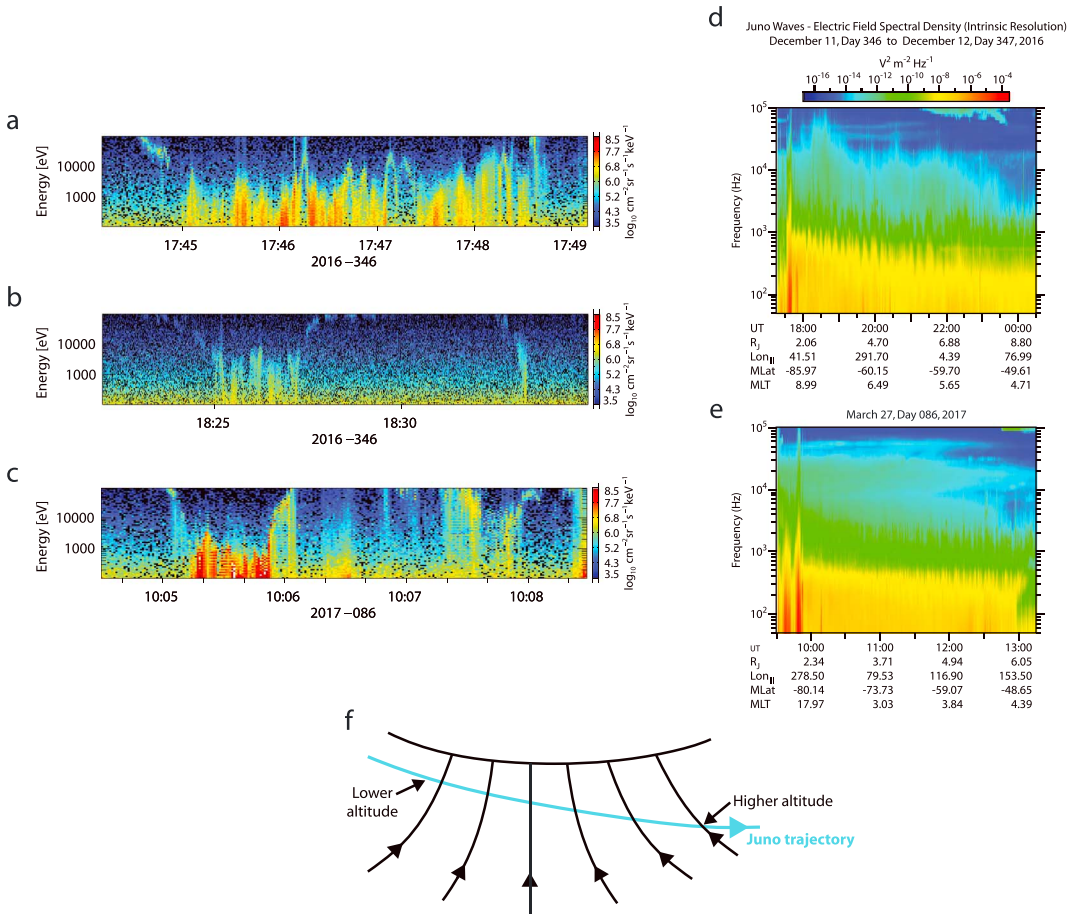

Figure 8. Juno JADE-E observations from the southern polar regions during perijove 3 (a, b) and perijove 5 (c). Characteristic inverted-V structures are observed in all three data sets (adapted from Ebert et al., 2017). Juno Waves observations of intense broadband whistler mode waves over the southern polar regions during perijove 3 (d) and perijove 5 (e). (f) Cartoon demonstrating the trajectory of Juno over the southern polar regions. Inverted-Vs were observed on perijove 3 and 5 when Juno was at lower altitudes (smaller radial distances).

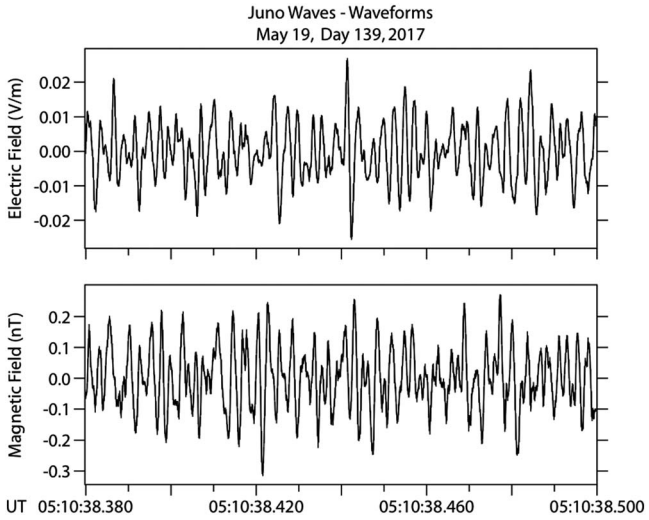

Figure 9. Example electric (top) and magnetic (bottom) waveforms for the northern polar region on perijove 6. The waves are electromagnetic but show signatures similar to ESWs. The irregularity in the electric field suggests possible stochastic electron acceleration.

et al., 2010). These soliton-like structures are also similar to whistler mode solitons, described in Treumann and Bernold (1981), which can contribute to stochastic electron acceleration. Even with a magnetic component, the irregularity in the waveforms and the broadband characteristic of the whistler mode waves suggests the development of chaotic field structures and associated stochastic electron acceleration. Using the electric field amplitude for these observed solitons (~0.02 V/m), and a propagation distance of one Jovian radii, we performed a simple calculation for the energy output, yielding approximately 1.4 MeV. Therefore, nearly relativistic energies may be achieved by acceleration by the solitons over just 1 R_J radial distance.

Another possible mechanism contributing to the stochastic acceleration of electrons is the upward sweep of the wave phase velocity (Figure 6b) with increasing altitude, which has the potential of carrying trapped electrons to high, relativistic, energies. Because of the higher density in the ionosphere, the whistler mode starts with low phase velocities in the inverted-V regions and thereafter increase up to nearly the speed of light as the waves propagate upward into lower density regions in the magnetosphere. Particles trapped in the wave can then be *swept* to

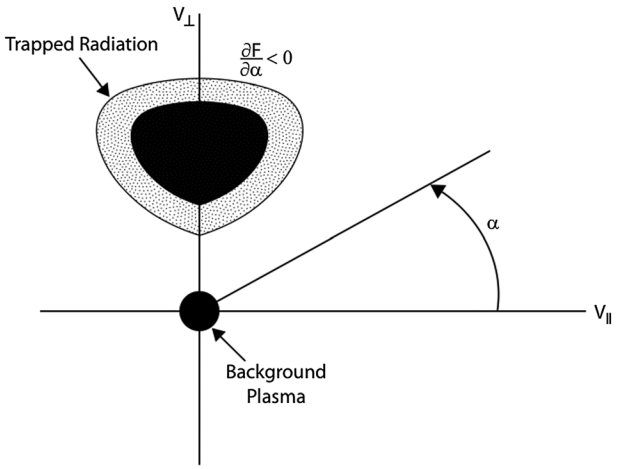

Figure 10. Distribution function for trapped radiation. The partial derivative term is negative, resulting in a positive growth rate.

high energies by the increasing phase velocity, as in a linear accelerator (Ashour-Abdalla, 1972; Kennel & Petschek, 1966; Matthews et al., 1984). Such trapping processes can result in a wide range of particle energies because of chaotic spiky variations in the electric field strengths, thereby resulting in power law-like energy spectrums.

We recognize the complicated nature of nonlinear effects and the overall stochastic acceleration mechanism, which we attribute to Hamiltonian chaos. To show that, the observed whistler mode electric field strengths and variations can account for the observed electron spectrums and intensities will require detailed computer simulations, but this is currently outside the scope of this paper. However, related simulations have been done on electrons trapped in the Jovian radiation belts. For example, Khazanov et al. (2007) conducted a study of high-energy electrons in the Jovian radiation belt to investigate local acceleration of electrons by whistler mode waves. This study used parameters that reflected typical whistler waves propagating in the radiation belt regions where the electron cyclotron frequency was both above and below the electron plasma frequency. They found that the resulting electron energies (from chaotic motions) were higher when the electron cyclotron frequency was higher than the electron plasma frequency. For this current study, the electron cyclotron frequency (~10^7 Hz) is higher than the estimated electron plasma frequency (~4×10^4 Hz) over the polar cap regions (Tetrick et al., 2017). This supports our general assertion that whistler mode waves can accelerate the electrons to very high energies through a stochastic process.

5. Comparison With Electron Acceleration in Radiation Belt Physics

It is important to note key differences between our proposed polar cap electron acceleration mechanism and the acceleration of trapped radiation belt electrons, which have been studied for several years (Horne & Thorne, 1998; Omura & Summers, 2006; Reeves et al., 2015; Summers et al., 2002; Thorne et al., 2013). Various mechanisms for accelerating electrons to high energies in Earth's radiation belts have been explored (e.g., Friedel et al., 2002). Among the different mechanisms, wave-particle interactions are a dominant way to accelerate electrons to high energies (Summers & Ma, 2000; Trakhtengerts et al., 2001). Electrons trapped in Earth's radiation belts interact with waves, leading to diffusion in both pitch angle and energy, resulting in electron acceleration (Summers & Ma, 2000). A study by Katoh and Omura (2004) showed that wave trapping is an effective way to accelerate electrons in Earth's radiation belts. In particular, whistler mode chorus waves have rising tones, which can extend the trapping region that guides some fraction of resonant electrons moving toward the equator, resulting in electron acceleration (Omura & Summers, 2006). Near the equator, electrons undergoing adiabatic mirror motion have the largest parallel velocities, but the mirror force decreases. Therefore, trajectories of resonant electrons are highly affected by parallel-propagating whistler mode waves (Omura & Summers, 2006). However, for the electrons to resonate with the waves, they must be moving in the opposite direction as the waves. This is called cyclotron resonance. In this paper, an entirely new type of interaction occurs between upward propagating electromagnetic whistler mode waves and upward traveling resonant electrons that can result in electron acceleration to high energies. This acceleration mechanism is new in the context of the Jovian polar cap region and because the Landau-type acceleration mechanism involved electromagnetic whistler mode waves.

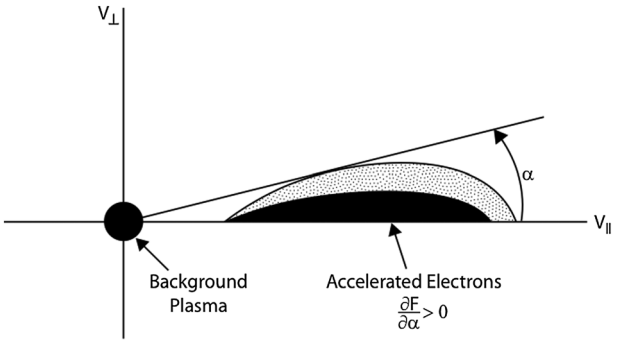

Figure 11. Resulting accelerated electron distribution function. A positive partial derivative term results in a negative growth rate, consistent with accelerated electrons.

To illustrate the difference between trapped radiation belt electrons and our polar cap electrons, we need to discuss the growth rate with both a typical electron distribution function for trapped radiation (Figure 10) and our distribution function for the resulting accelerated polar cap electrons (Figure 11). To do this comparison, it is

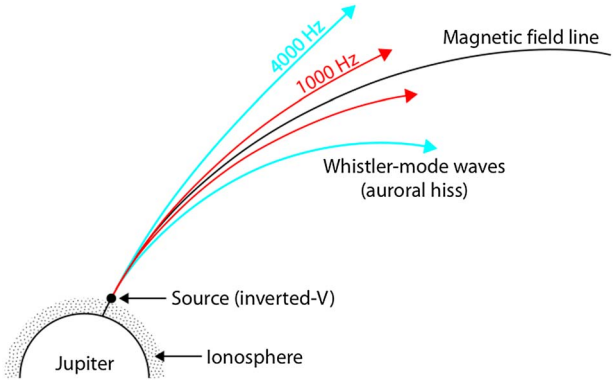

Figure 12. Assumed location of inverted-Vs (just above the ionosphere), generating whistler mode waves. Example ray paths for 1000 and 4000 Hz shown, demonstrating the frequency dependence of wave propagation. The deviation from the magnetic field is caused by wave propagation near the resonance cone (typical of whistler mode auroral hiss).

useful to rewrite the growth rate equation (equation (1)) in terms of the pitch angle, α (Gurnett & Bhattacharjee, 2017), as originally derived by Kennel and Petschek (1966) the following:

$$\frac{\gamma}{\omega_c} = \pi\left(1-\frac{\omega}{\omega_c}\right)^2\left[-\frac{\omega}{|k_\parallel|}\int_0^\infty F_0 2\pi v_\perp + \frac{k_\parallel}{|k_\parallel|}\int_0^\infty\left(-\frac{\partial F_0}{\partial\alpha}\right)\pi v_\perp^2 dv_\perp\right]\Bigg|_{v_\parallel = v_{\parallel \mathrm{Res}}} \quad (3)$$

The important instability term, which has now been written as a function of pitch angle, is $-\partial F_0/\partial\alpha$ (equation (3)). Writing the growth rate equation in terms of pitch angle is typical for radiation belt physics. Analysis of the electrons accelerated over the Jovian polar cap (Figure 11) shows that the instability term is positive, resulting in a negative γ. This result is consistent with our previous results that showed wave damping and electron acceleration. In contrast, for the typical loss cone distribution of trapped radiation electrons (Figure 10), the instability term is negative, resulting in a positive γ and hence, a cyclotron instability. This comparison is consistent with Elliott et al. (2018), which compared the pitch angle scattering of the upward traveling electrons in the polar cap to typical pitch angle scattering of radiation belt electrons and found that the upward traveling electrons were scattered away from the magnetic field line. This result showed how different the Jovian polar cap is compared to typical radiation belts.

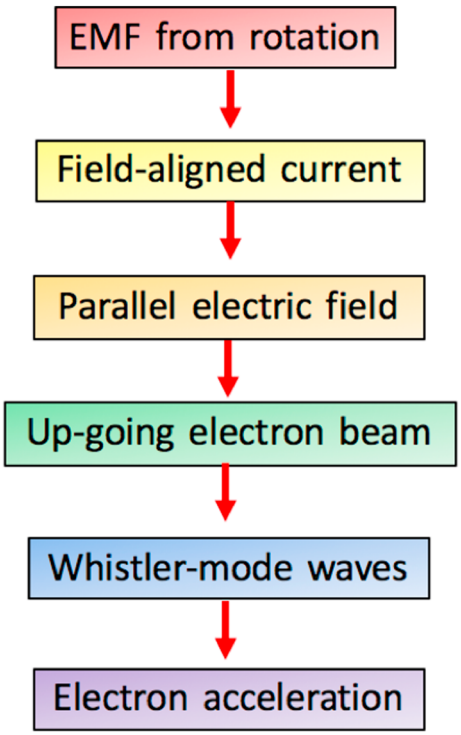

Figure 13. Flow chart representing the important steps in our proposed acceleration process. First, an electromotive force is induced from the rapid rotation of Jupiter. This electromotive force then produces a field-aligned current that points downward in the polar cap. When the plasma cannot carry the current, a parallel electric field develops, which in turn causes a beam of upward traveling electrons. This electron beam causes an $n = 0$ instability to occur, resulting in upward propagating whistler mode waves. Lastly, as the phase velocity of the waves exceeds the beam velocity, the energy from the waves goes into accelerating the electrons.

6. Conclusions

We propose a mechanism to explain the acceleration of upward traveling electrons in the Jovian polar cap. We believe that a downward field-aligned current over the polar cap, ultimately driven by the rotation of Jupiter, generates strong downward parallel electric fields and upgoing electron beams in the low-density regions of Jupiter's upper ionosphere. The upward traveling electrons produce intense upward propagating whistler mode waves over a broad range of frequencies via a beam-plasma instability. Figure 12 shows the assumed source region (just above the ionosphere), where an inverted-V occurs, generating the whistler mode waves. As the whistler mode waves propagate upward along the magnetic field lines to higher altitudes, the waves are absorbed by nonlinear velocity space diffusion processes (Hamiltonian chaos) that act to stochastically accelerate the resonant electrons to high energies. A characteristic signature of Hamiltonian chaos is observed in the whistler mode electric fields as spiky soliton-like variations. The rapid increase in the phase velocity of the whistler mode waves with increasing altitude can also cause electrons trapped in the wavefield to be accelerated to velocities approaching the speed of light. A flow chart that demonstrates the important steps in our proposed acceleration mechanism is shown in Figure 13. The work presented in this paper has addressed the question of the main cause of the stochastic electron acceleration, which was posed in Mauk et al. (2018). This work has demonstrated how upward traveling electrons can interact and be accelerated by upward propagating electromagnetic whistler mode waves, resulting in a wide range of electron energies. Our proposed acceleration mechanism will create a platform for simulation models to prove that such wave-particle interactions can result in the observed electron energies.

Appendix A

Here we show that the first two important terms in equation (1) cancel out when the $n = 0$ resonance condition is considered. The two terms of interest are as follows:

$$-\frac{\omega}{|k_\parallel|}\int_0^\infty F_0 2\pi v_\perp \mathrm{d}v_\perp \tag{A1}$$

$$-\int_0^\infty \left(v_\parallel \frac{\partial F_0}{\partial v_\perp}\right)\pi v_\perp^2 \mathrm{d}v_\perp \tag{A2}$$

We will conduct integration by parts on the second term using the following resonance condition:

$$v_\parallel = v_{\parallel \mathrm{Res}} = \frac{\omega}{k_\parallel} \tag{A3}$$

The following is the integration of the second term:

$$-\int_0^\infty \left(v_\parallel \frac{\partial F_0}{\partial v_\perp}\right)\pi v_\perp^2 \mathrm{d}v_\perp \Big|_{v_\parallel = \frac{\omega}{k_\parallel}} \tag{A4}$$

$$= -v_\parallel \int_0^\infty \left(\frac{\partial F_0}{\partial v_\perp}\right)\pi v_\perp^2 \mathrm{d}v_\perp \Big|_{v_\parallel = \frac{\omega}{k_\parallel}} \tag{A5}$$

LET

$$u = \pi v_\perp^2$$
$$\mathrm{d}u = 2\pi v_\perp \mathrm{d}v_\perp$$
$$\mathrm{d}v = \frac{\partial F_0}{\partial v_\perp}$$
$$v = F_0$$

Carrying out integration by parts ($uv - \int v\mathrm{d}u$), we get the following:

$$-v_\parallel \left(\pi v_\perp^2 F_0 - \int F_0 2\pi v_\perp \mathrm{d}v_\perp\right) \tag{A6}$$

where the second term, $v_\parallel \int F_0 2\pi v_\perp \mathrm{d}v_\perp$, using our resonance condition, gives us the following:

$$+\frac{\omega}{k_\parallel}\int F_0 2\pi v_\perp \mathrm{d}v_\perp \tag{A7}$$

which exactly cancels the first important term in equation (1) as follows:

$$-\frac{\omega}{|k_\parallel|}\int_0^\infty F_0 2\pi v_\perp \mathrm{d}v_\perp \tag{A8}$$

Acknowledgments
The research at the University of Iowa was supported by NASA through contract 699041X with the Southwest Research Institute. We thank both Jack Connerney and Robert Mutel for their helpful feedback and suggestions. Juno data are regularly made publicly available via the Planetary Data System (https://pds.jpl.nasa.gov) according to the Juno Project archiving schedule.

References

Allegrini, F., Bagenal, F., Bolton, S., Connerney, J., Clark, G., Ebert, R. W., et al. (2017). Electron beams and loss cones in the auroral regions of Jupiter. *Geophysical Research Letters*, *44*, 7131–7139. https://doi.org/10.1002/2017GL073180

Ashour-Abdalla, M. (1972). Amplification of whistler waves in the magnetosphere. *Planetary and Space Science*, *20*(5), 639–662, https://doi.org/10.1016/0032-0633(72)90151-1

Biswas, A., Daniela, M., & Zerrad, E. (2010). An exact solution for electromagnetic solitons in relativistic plasmas. *Physica Scripta*, *81*(2), 025506. https://doi.org/10.1088/0031-8949/81/02/025506

Chapman, S. (1931). The absorption and dissociative or ionizing effect of monochromatic radiation in an atmosphere on a rotating Earth part II. *Proceedings of the Physical Society*, *43*(5), 483–501. https://doi.org/10.1088/0959-5309/43/5/302

Clark, G., Mauk, B. H., Haggerty, D., Paranicas, C., Kollmann, P., Rymer, A., et al. (2017). Energetic particle signatures of magnetic field-aligned potentials over Jupiter's polar regions. *Geophysical Research Letters*, *44*, 8703–8711. https://doi.org/10.1002/2017GL074366

Connerney, J. E. P. (1981). Azimuthal magnetic field at Jupiter: Comment on the paper by J. L. Parish, C. K. Goertz, and M. F. Thomsen. *Journal of Geophysical Research*, *86*(A9), 7796–7797. https://doi.org/10.1029/JA086iA09p07796

Connerney, J. E. P., Adriani, A., Bagenal, F., Bolton, S. J., Cowley, S., Gerard, J.-C., et al. (2017). Jupiter's magnetosphere and aurora observed by the Juno spacecraft during its first polar pass. *Science*, *356*(6340), 826–832. https://doi.org/10.1126/science.aam5928

Ebert, R. W., Allegrini, F., Bagenal, F., Bolton, S. J., Connerney, J. E. P., Clark, G., et al. (2017). Spatial distribution and properties of 0.1–100 keV electrons in Jupiter's polar auroral region. *Geophysical Research Letters*, *44*, 9199–9207. https://doi.org/10.1002/2017GL075106

Elliott, S. S., Gurnett, D. A., Kurth, W. S., Clark, G., Mauk, B. H., Bolton, S. J., et al. (2018). Pitch angle scattering of up-going electron beams in Jupiter's polar regions by whistler-mode waves. *Geophysical Research Letters*, *45*, 1246–1252. https://doi.org/10.1002/2017GL076878

Ergun, R. E., Carlson, C. W., McFadden, J. P., Mozer, F. S., Delory, G. T., Peria, W., et al. (1998). FAST satellite observations of large-amplitude solitary structures. *Geophysical Research Letters*, *25*(12), 2041–2044. https://doi.org/10.1029/98GL00636

Frank, L. A., & Ackerson, K. L. (1971). Observations of charged particle precipitation into the auroral zone. *Journal of Geophysical Research*, *76*(16), 3612–3643. https://doi.org/10.1029/JA076i016p03612

Friedel, R. H. W., Reeves, G. D., & Obara, T. (2002). Relativistic electron dynamics in the inner magnetosphere: A review. *Journal of Atmospheric and Solar - Terrestrial Physics*, *64*(2), 265–282. https://doi.org/10.1016/S1364-6826(01)00088-8

Gurnett, D. A. (1972). Electric field and plasma observations in the magnetosphere (pp. 123–138). In B. E. R. Dyer (Ed.), *Critical problems of magnetospheric physics, Proceedings of the Symposium Jointly Sponsored by COSPAR, IAGA, and URSI, May 11–13, 1972 in Madrid, Spain*, Washington, DC: National Academy of Sciences.

Gurnett, D. A., & Bhattacharjee, A. (2017). *Introduction to plasma physics with space and laboratory applications*. Cambridge, UK: Cambridge University Press.

Gurnett, D. A., & Frank, L. A. (1972). VLF hiss and related plasma observations in the polar magnetosphere. *Journal of Geophysical Research*, *77*(1), 172–1190. https://doi.org/10.1029/JA077i001p00172

Gurnett, D. A., Shawhan, S. D., & Shaw, R. R. (1983). Auroral hiss, Z more radiation, and auroral kilometric radiation in the polar magnetosphere: DE 1 observations. *Journal of Geophysical Research*, *88*(A1), 329–340. https://doi.org/10.1029/JA088iA01p00329

Hill, T. W. (1979). Inertial limit on corotation. *Journal of Geophysical Research*, *84*(A11), 6554–6558. https://doi.org/10.1029/JA084iA11p06554

Horne, R. B., & Thorne, R. M. (1998). Potential waves for relativistic electron scattering and stochastic acceleration during magnetic storms. *Geophysical Research Letters*, *25*(15), 3011–3014. https://doi.org/10.1029/98GL01002

Katoh, Y., & Omura, Y. (2004). Acceleration of relativistic electrons due to resonant scattering by whistler mode waves generated by temperature anisotropy in the inner magnetosphere. *Journal of Geophysical Research*, *109*, A12214. https://doi.org/10.1029/2004JA010654

Kennel, C. F., & Petschek, H. E. (1966). Limit on stably trapped particle fluxes. *Journal of Geophysical Research*, *71*(1), 1–28. https://doi.org/10.1029/JZ071i001p00001

Kennel, C. F., & Wong, H. V. (1967). Resonant particle instabilities in a uniform magnetic field. *Journal of Plasma Physics*, *1*(01), 75. https://doi.org/10.1017/S0022377800003111

Khazanov, G. V., Tel'nikhin, A. A., & Kronberg, T. K. (2007). Chaotic motion of relativistic electrons driven by whistler waves. *Plasma Physics and Controlled Fusion*, *49*(4), 447–466. https://doi.org/10.1088/0741-3335/49/4/008

Kurth, W. S., Hospodarsky, G. B., Kirchner, D. L., Mokrzycki, B. T., Averkamp, T. F., Robison, W. T., et al. (2017). The Juno Waves investigation. *Space Science Reviews*, *213*(1-4), 347–392. https://doi.org/10.1007/s11214-017-0396-y

Ma, C., & Summers, D. (1998). Formation of power-law energy spectra in space plasmas by stochastic acceleration due to whistler-mode waves. *Geophysical Research Letters*, *25*(21), 4099–4102. https://doi.org/10.1029/1998GL900108

Matsumoto, H., Kojima, H., Miyatake, T., Omura, Y., Okada, M., Nagano, I., & Tsutsui, M. (1994). Electrostatic solitary waves (ESW) in the magnetotail: BEN wave forms observed by Geotail. *Geophysical Research Letters*, *21*(25), 2915–2918. https://doi.org/10.1029/94GL01284

Matthews, J. P., Omura, Y., & Matsumoto, H. (1984). A study of particle trapping by whistler mode waves in the geomagnetic field: The early development of the VLF quiet band. *Journal of Geophysical Research*, *89*(A4), 2275–2287. https://doi.org/10.1029/JA089iA04p02275

Mauk, B. H., Haggerty, D. K., Jaskulek, S. E., Schlemm, C. E., Brown, L. E., Cooper, S. A., et al. (2017). The Jupiter Energetic Particle Detector Instrument (JEDI) investigation for the Juno mission. *Space Science Reviews*, *213*(1-4), 289–346. https://doi.org/10.1007/s11214-013-0025-3

Mauk, B. H., Haggerty, D. K., Paranicas, C., Clark, G., Kollmann, P., Rymer, A. M., et al. (2017). Juno observations of energetic charged particles over Jupiter's polar regions: Analysis of mono- and bi-directional electron beams. *Geophysical Research Letters*, *44*, 4410–4418. https://doi.org/10.1002/2016GL072286

Mauk, B. H., Haggerty, D. K., Paranicas, C., Clark, G., Kollmann, P., Rymer, A. M., et al. (2018). Diverse electron and ion acceleration characteristics observed over Jupiter's main aurora. *Geophysical Research Letters*, *45*, 1277–1285. https://doi.org/10.1002/2017GL076901

McComas, D. J., Alexander, N., Allegrini, F., Bagenal, F., Beebe, C., Clark, G., et al. (2017). The Jovian Auroral Distributions Experiment (JADE) on the Juno mission to Jupiter. *Space Science Reviews*, *213*(1-4), 547–643. https://doi.org/10.1007/s11214-013-9990-9

Mozer, F. S., Agapitov, O., Krasnoselskikh, V., Lejosne, S., Reeves, G. D., & Roth, I. (2014). Direct observations of radiation-belt electron acceleration from electron-volt energies to megavolts by nonlinear whistlers. *Physical Review Letters*, *113*(3), 035001. https://doi.org/10.1103/PhysRevLett.113.035001

Mozer, F. S., Ergun, R., Temerin, M., Cattell, C., Dombeck, J., & Wygant, J. (1997). New features of time domain electric field structures in the auroral acceleration region. *Physical Review Letters*, *79*(7), 1281–1284. https://doi.org/10.1103/PhysRevLett.79

Mozer, F. S., & Hull, A. (2001). Origin and geometry of upward parallel electric fields in the auroral acceleration region. *Journal of Geophysical Research*, *106*(A4), 5763–5778. https://doi.org/10.1029/2000JA900117

Omura, Y., & Summers, D. (2006). Dynamics of high-energy electrons interacting with whistler mode chorus emissions in the magnetosphere. *Journal of Geophysical Research*, *111*, A09222. https://doi.org/10.1029/2006JA011600

Paranicas, C., Mauk, B. H., Haggerty, D. K., Clark, G., Kollmann, P., Rymer, A. M., et al. (2018). Intervals of intense energetic electron beams over Jupiter's poles. *Journal of Geophysical Research: Space Physics*, *123*, 1989–1999. https://doi.org/10.1002/2017JA025106

Pugh, E. M., & Pugh, E. W. (1965). *Principles of electricity and magnetism*. Reading, Massachusetts, U.S.A: Addison-Wesley Publishing Company, Inc.

Reeves, G. D., Friedel, R. H. W., Larsen, B. A., Skoug, R. M., Funsten, H. O., Claudepierre, S. G., et al. (2015). Energy-dependent dynamics of keV to MeV electrons in the inner zone, outer zone, and slot regions. *Journal of Geophysical Research: Space Physics*, *121*, 397–412. https://doi.org/10.1002/2015JA021569

Summers, D., & Ma, C. (2000). A model for generating relativistic electrons in the Earth's inner magnetosphere based on gyroresonant wave-particle interactions. *Journal of Geophysical Research*, *105*(A2), 2625–2639. https://doi.org/10.1029/1999JA900444

Summers, D., Ma, C., Meredith, N. P., Horne, R. B., Thorne, R. M., Heynderickx, D., & Anderson, R. R. (2002). Model of the energization of outer-zone electrons by whistler-mode chorus during the October 9, 1990 geomagnetic storm. *Geophysical Research Letters*, *29*(24), 2174. https://doi.org/10.1029/2002GL016039

Temerin, M., Cerny, K., Lotko, W., & Mozer, F. S. (1982). Observations of double layers and solitary waves in the auroral plasma. *Physical Review Letters*, *48*(17), 1175–1179. https://doi.org/10.1103/PhysRevLett.48.1175

Tetrick, S. S., Gurnett, D. A., Kurth, W. S., Imai, M., Hospodarsky, G. B., Bolton, S. J., et al. (2017). Plasma waves in Jupiter's high latitude regions: Observations from the Juno spacecraft. *Geophysical Research Letters*, *44*, 4447–4454. https://doi.org/10.1002/2017GL073073

Thorne, R. M., Li, W., Ni, B., Ma, Q., Bortnik, J., Chen, L., et al. (2013). Rapid local acceleration of relativistic radiation belt electrons by magnetospheric chorus. *Nature*, *504*(7480), 411–414. https://doi.org/10.1038/nature12889

Trakhtengerts, V. Y., Hobara, Y., Demekhov, A. G., & Hayakawa, M. (2001). A role of the second-order cyclotron resonance effect in a self-consistent approach to triggered VLF emissions. *Journal of Geophysical Research*, *106*(A3), 3897–3904. https://doi.org/10.1029/2000JA000025

Treumann, R., & Bernold, T. E. X. (1981). Radiation from a whistler soliton in interaction with a plasma wave. *Physical Review Letters*, *47*(20), 1455–1458. https://doi.org/10.1103/PhysRevLett.47